Hydrogeological properties of geosynthetic clay liners (GCL) permeated with synthetic acid mine drainage

Cheve N., Bussière B.
Research Institute on Mines and the Environment, Université du Québec en Abitibi-Témiscamingue, Rouyn-Noranda, Québec, Canada

ABSTRACT
The performance of a conventional geosynthetic clay liner (GCL) acting as a barrier to fluids responsible for generating acid mine drainage was investigated in the laboratory. To do so, the saturated hydraulic conductivities (k_{sat}), the drying water retention curves, and the effective diffusion coefficients (D_e) were compared for GCL specimens hydrated under low confining pressures with either deionized water or with synthetic acid mine drainage (SAMD). Hydration with SAMD led to k_{sat} values approximately 10 times higher than those of samples hydrated with deionized water. Little to no impacts were observed on the water retention curves or D_e values. However, for a given D_e, the diffusive flux of oxygen through a GCL hydrated with SAMD was higher than for one hydrated with deionized water because the samples hydrated with the SAMD were 15 to 20 % thinner. Thus, permeation with SAMD adversely affected the performance of the studied GCL.

RÉSUMÉ
L'influence d'une hydratation au drainage minier acide sur les propriétés hydrogéologiques d'un géocomposite bentonitique (GCB) conventionnel a été étudiée au laboratoire. Pour se faire, la conductivité hydraulique saturée, la courbe de rétention d'eau en drainage et le coefficient de diffusion effectif d'échantillons de GCB hydratés à l'eau déionisée et au drainage minier acide synthétique (DMAS) à de faibles pressions de confinement ont été comparés. L'hydratation au DMAS a mené à une conductivité hydraulique saturée environ 10 fois plus élevée que celle des échantillons hydratés à l'eau déionisée, tandis que les impacts observés sur la courbe de rétention d'eau et le coefficient de diffusion effectif ont été moindre. Toutefois, pour un même coefficient de diffusion effectif, le flux diffusif d'oxygène au travers d'un GCB hydraté au DMAS s'avère plus élevé que pour une hydratation à l'eau déionisée puisque les échantillons hydratés au DMAS sont de 15-20% plus minces. Ainsi, l'hydratation au DMAS a eu un effet négatif sur la performance du GCB à l'étude.

1 INTRODUCTION

Sulphide mine wastes exposed to water and oxygen can oxidize and generate acid mine drainage (AMD), which is typically characterized by low pH values and high dissolved metal and sulfate concentrations (e.g. Akcil and Koldas 2006; Blowes et al. 2014; Moncur et al. 2005). A wide variety of methods have been developed to prevent and control the production of AMD and thus limit associated environmental problems. One method that is frequently suggested is the construction of a multi-layered engineered cover over the mine wastes (Aubertin et al. 2016; INAP 2012). In such covers, one layer is usually made of a low saturated hydraulic conductivity (k_{sat}) material that limits the infiltration of water and/or the migration of oxygen into the reactive wastes. Commonly used materials in this layer include fine-grained soils, low sulfide tailings, and geomembranes, however, these materials may not always be available or economically viable.

Presently, geosynthetic clay liners (GCLs) are increasingly being considered as an alternative low-k_{sat} material for engineered covers. GCLs are thin (~ 5 - 10 mm), manufactured sheets that consist of a layer of bentonite interlaid between two geotextiles. Interest in the material is mainly due to its ease of installation, low k_{sat} and ability to self-heal cracks and perforations when permeated with deionized water or low ionic strength solutions (Bouazza 2002; Daniel et al. 1997; Eigenbrod 2003; Lange et al. 2007; Melchior 2002; Sari and Chai 2013; Sivakumar Babu et al. 2001). However, hydration or permeation of bentonite with solutions containing multivalent inorganic cations, such as those prevalent in AMD, usually result in changes in the chemistry of the bentonite; i.e. the monovalent Na^+ cations of the bentonite are replaced by multivalent cations, which results in less swelling and higher hydraulic conductivities (Egloffstein 2001; Mesri and Olson 1971; Shackelford 1994; Shackelford et al. 2010; Shackelford et al. 2000).

Many studies have assessed the effects of various liquids on cation exchanges and the properties of interest of GCLs. However, relatively little information is available about the effects of permeating a GCL with AMD, particularly with respect to the parameters of interest in a multi-layered engineered mine cover. Therefore, the main objective of this study was to determine the effects of AMD on the capacity of a GCL to act as a barrier to water and oxygen. The main parameters investigated in this laboratory study were the k_{sat}, the water retention curve (WRC), and the effective diffusion coefficient (D_e) for GCL specimens permeated with deionized water (DIW) or synthetic acid mine drainage (SAMD).

2 MATERIALS AND METHODS

2.1 Materials

2.1.1 Geosynthetic clay liner

The GCL tested in this study consisted of a layer of fine, granular bentonite interlaid between a non-woven and a reinforced non-woven geotextile that was assembled by a needle-punch process and thermally treated. GCL rolls (4.72 m × 45.72 m) were shipped to a nearby mine site for installation; then a ~3-m long sample was taken from one of the rolls for laboratory testing. The 3-m long sample was divided into 45 cm × 45 cm sub-samples and stored in laboratory until testing. The initial thickness of the GCL sample was measured at ten locations on various sub-samples and values ranged from 6.5 to 6.9 mm.

The average mass per unit area was 240 g/m², 260 g/m², and 5200 g/m² for the top and bottom geotextiles, and for the oven-dried bentonite, respectively. The specific gravity (G_s) of the geotextiles and the bentonite was measured using a gas pycnometer (UltraPyc 1200e, Quantachrome Instruments) following the ASTM D5550 protocol (ASTM 2014). Average values of 0.97 and of 2.51 were obtained for the geotextiles and the bentonite, respectively. The overall G_s of the GCL was estimated to be 2.20 based on measurements performed on five dry specimens (see Chevé 2019 for more details).

X-ray diffraction (XRD) analyses were performed by an external laboratory on two sub-samples of bentonite. Diffractograms were analyzed using the TOPAS software, implementing a Reitveld refinement to reconcile the mineralogical quantification with the bulk chemistry (Bruker 2009). The results from the semi-quantitative analysis indicated that the bentonite contained an average of 65% smectite minerals (~35% montmorillonite and 30% beidellite), 15% quartz and cristobalite, 12% albite, 4% K-feldspar, 2 % calcite, and trace amounts of other minerals.

2.1.2 Synthetic acid mine drainage

Tests were conducted on five GCL specimens with two different permeants liquids: de-aired deionized water (DIW) and synthetic acid-mine drainage (SAMD). Deionized water was used with GCL 13, 18, 23, and 24 to establish benchmark results. GCL 20, 21, and 22 were hydrated and permeated with SAMD to represent a worst-case scenario corresponding to a GCL that hydrates solely by the uptake of AMD. In the following section, the suffices “DI” and “SA” are used to identify the specimens permeated with DIW and SAMD, respectively.

The SAMD was prepared based on chemical analyses of a reference AMD sample (AMD_{ref}) collected from an active gold mine. The water quality of AMD_{ref} is typical of other samples presented in the literature (e.g. Blowes et al. (2014); Lindsay et al. (2015)). The SAMD was prepared using DIW, salts, dolomite powder, and nitrate solutions. The compounds used for the SAMD preparation and the average measured elemental concentrations are shown in Table 1. The SAMD had a pH of 2.4, and Fe and sulfate concentrations of 2.25 g/L and 9.06 g/L, respectively. Al, Ca, Mn, and Zn were present in concentrations ranging from 100-550 mg/L.

Table 1. Chemical and electrochemical properties of synthetic acid mine drainage (SAMD).

Parameter	Source in SAMD	SAMD
Aluminium (Al)	$AlCl3 \cdot 6\ H_2O$	128 mg/l
Calcium (Ca)	$CaMg(CO_3)_2$	547 mg/l
Copper (Cu)	$CuNO_3$	7.6 mg/l
Iron (Fe)	$Fe2(SO_4)_3 \cdot H_2O$	1930 mg/l
Magnesium (Mg)	$CaMg(CO_3)_2$	392 mg/l
Manganese (Mn)	$MnNO_3$	11.3 mg/l
Potassium (K)	KNO_3	7.8 mg/l
Sodium (Na)	$NaNO_3$	11.3 mg/l
Sulfur (S)	$Fe_2(SO_4)3 \cdot H_2O$ $Zn(SO_4) \cdot 7H_2O$	3020 mg/l
Zinc (Zn)	$Zn(SO_4) \cdot 7H_2O$	142 mg/l
pH	---	2.4
Electrical conductivity (EC)	---	8.7 mS/cm
RMD	---	0.004 $M^{½}$
Ionic strength (I)	---	0.83 M

2.2 Methods

2.2.1 Permeability test

GCLs were prepared by cutting circular specimens with a diameter of 100 ± 1 mm in the center of randomly selected sub-samples with a precision knife. DIW or SAMD was applied along the cutting line of the circular specimen to wet the bentonite at the edge and minimize bentonite loss during preparation.

The k_{sat} values were determined in flexible-wall permeameters based on the ASTM D5887 (ASTM 2016) and ASTM D6766 (ASTM 2012) protocols for tests using DIW and SAMD. The permeability tests were conducted using the falling headwater, rising tailwater elevation method. Low backpressure and effective stress were used during the permeability tests to simulate conditions representative of a GCL in a cover system (Makusa et al. 2014; Meer and Benson 2007; Rowe and Hosney 2013; Scalia and Benson 2010) and to avoid a lower k_{sat} associated with the default pressures of the ASTM 6766 method (Conzelmann et al. 2017). An initial average effective stress of 27.5 kPa was applied to the specimen using a cell pressure of 38.0 ± 2.0 kPa, a backpressure of 3.0 ± 2.0 kPa, and a base pressure of 18.0 ± 2.0 kPa. The average effective stress varied from 26.5 kPa to 31.1 kPa because of the nature of the selected test protocol (falling headwater, rising tailwater) and the variation in thickness during permeation. Uncertainty on the k_{sat} measurements was estimated to range from 30 to 50% (Daniel et al. 1997; Koerner 2004). Permeation of all specimens was carried out until ASTM D5887 and ASTM D6766 termination criteria were reached.

The diameter and height (h) of the GCL specimens were also measured after the permeability tests using a digital calliper with an accuracy of ± 0.01 mm. Diameters were measured at four locations and heights at eight

locations. Specimen were also weighed after the completion of a permeability test.

2.2.2 Water retention curves

The water retention curve of a GCL covers a wide range of suctions. Therefore, three methods were combined to determine the moisture (ω) – suction (ψ) characteristics of the GCL. A 100-bar pressure membrane extractor (Soilmoisture Equipment Corp.) was used for low suctions (< 1.5 MPa) while vapor desiccators with saturated salt solutions and WP4C device (METER Group) were used for high suctions (> 1 MPa).

The pressure membrane extractor test was conducted on specimen GCL 18DI. The sample was removed from the permeability cell after saturation, then placed without any loading on a saturated cellulose membrane of the pressure extractor. Tests were run at an applied pressure of 0.10 and 0.51 MPa following Method C of ASTM D6836. For each test, the pressure was applied until mass equilibrium was reached (7 to 8 days).

GCL18DI was used for a diffusion test (section 2.2.3) then split in two. Each half specimen was placed in a desiccator containing a saturated salt solution of $CuSO_4$ or KNO_3. The relative humidity (RH) of these solutions was estimated at 98.0% and 96.2% (Wexler and Hasegawa 1954; Young 1967), respectively, which corresponds to suctions of 2.8 and 10.5 MPa based on Kelvin's equation (with an average temperature of 23°C recorded during the tests). Each test was carried out until mass equilibrium was reached. The test with $CuSO_4$ solution lasted 109 days, while the one with KNO_3 solution lasted 69 days.

Specimens GCL20SA and GCL23DI were used for measurements with the WP4C device. This apparatus uses the chilled-mirror dew-point method (ASTM D6836, Method D) to determine the soil suction of a specimen at a certain water content. Suction can be measured from 1-300 MPa, with a resolution of ± 0.1 MPa (Devices 2010). Details on the use of the WP4C to determine the WRC of a GCL can be found in Lu et al. (2017); and Rouf et al. (2016). Each tested specimen was divided into three 38-mm diameter sub-specimens in order to fit in the sample cup of the device. After a reading with the WP4C, a sub-specimen was weighed and measured. It was then placed in the oven at 105°C until a mass loss of at least 0.3 g was measured, then wrapped in a cellophane paper, transferred to a 4°C refrigerator for ± 30 minutes, and finally kept at room temperature for at least 3-4 hours. A total of 15 measurements were made on the three subsamples of GCL20SA and 14 measurements on the subsamples of GCL23DI. Each reading with the WP4C lasted between 2 to 4 hours.

The diameter and height of the GCL specimens were measured at the end of each test conducted with the pressure extractor and the WP4C device. A $S_r(\psi)$ relationship was determined based on the estimated G_s of the GCL and the measured dimensions. This conversion was made because, for compressible materials such as GCLs, the WRC and its associated air entry value (AEV) are better defined when using a $S_r(\psi)$ relationship (Mbonimpa et al. 2006; Wijaya et al. 2015).

2.2.3 Diffusion

In highly saturated porous soils (S_r > 80-85%), the main gas migration mechanism is diffusion (Collin 1987). For 1D gas diffusion, the oxygen flux can be determined with Fick's first law (Equation 1) (Crank 1975; Cussler 2009):

$$F(z,t) = -D_e \frac{\partial C(z,t)}{\partial z} \quad [1]$$

where F is the diffusive flux, D_e is the effective diffusion coefficient of oxygen (O_2) through the porous medium, C is the O_2 concentration, z is the depth, and t is time.

The D_e of GCL 13DI, 18DI, 20SA, and 22SA was estimated with the predictive model developed by Aachib and al. (2002, 2004) (equation 2):

$$D_e = \frac{1}{n^2}(D_a^0 \theta_a^{pa} + H D_w^0 \theta_w^{pw}) \quad [2]$$

where n is the porosity, D_a^0 and D_w^0 are the free diffusion coefficients of O_2 in air and in water (1.8 x 10^{-5} m²/s and 2.5 x 10^{-9} m²/s at 20°C), θ_a and θ_w are the volumetric water contents of air and water in the soil, p_a and p_w are parameters related to tortuosity of air and water (≈ 3.4).

The D_e was thereafter determined with oxygen diffusion tests performed in a diffusion cell similar to the one used by Aubertin et al. (2000) (Figure 1). It consists of a PVC cylinder with an internal diameter of 10 cm and a length of 30 cm, with two reservoirs separated by the porous medium to be analyzed. Layers of sand with a low AEV were installed on each side of the GCL in order to produce a capillary break and limit the desaturation of the GCL during the experiment. An oxygen sensor (SO-110, Apogee Instruments) was fixed at the end of each reservoir to measure the evolution of the oxygen concentration along the test. Both sensors were connected to a Hobo UX120 data logger (Onset Computer Corporation) and were calibrated before each test in the open air and in pure nitrogen.

The experimental procedure is based on a closed system, where the O_2 concentration in the source reservoir decreases over time, while the concentration in the receptor reservoir increases proportionally to the diffusive flux (Aubertin et al. 2000). After purging both reservoirs with humidified nitrogen, the source reservoir was briefly opened to reach atmospheric conditions (~ 8.3 mol/m³) (Aachib et al. 2002). The temporal evolution of the O_2 concentration in each reservoir was then recorded at time steps varying from 1 to 10 minutes. The tests were carried out until a similar O_2 concentration was measured in the source and the receptor reservoir, which took from 3 to 9 days depending on the degree of saturation of the tested GCL.

The POLLUTEv7 software (GAEA Technologies) was used to determine the D_e of each GCL by iteratively fitting the measured results with simulated ones. More details on the interpretation of results can be found in Mbonimpa et al. (2002) and Aachib et al. (2004).

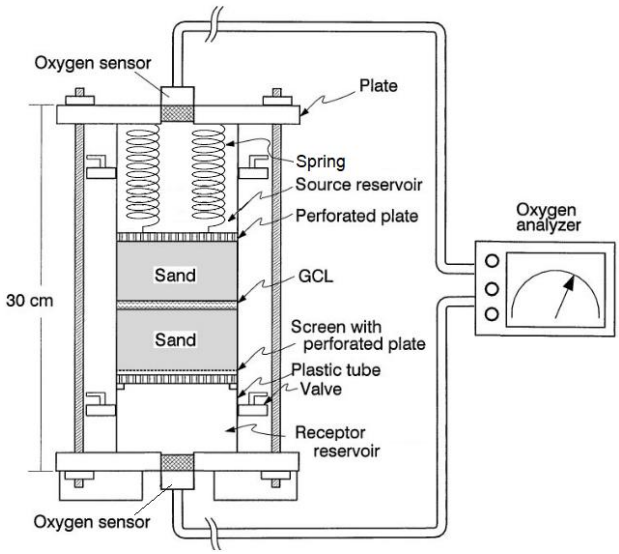

Figure 1. Schematic representation of the diffusion cells (adapted from Aubertin et al. (2000)).

3 RESULTS

3.1 Permeability tests

Results from the permeability tests are presented in Table 2. Phase relationships indicated that a degree of saturation > 95% was reached for all specimens, apart from GCL13DI, at the end of the permeability tests. The measured k_{sat} values of specimens permeated with DIW was approximately one order of magnitude smaller than those for specimens permeated with SAMD; average values were 3.3×10^{-9} cm/s and 2.2×10^{-8} cm/s, respectively. Furthermore, specimens saturated with DIW were ~15-20% thicker than those saturated with SAMD by the end of the tests.

Table 2. Permeability tests results.

Specimen	k_{sat} (cm/s)	Average final thickness (mm)
GCL 13DI	6.5×10^{-10} (1)	9.5
GCL 18DI	3.9×10^{-9}	9.5
GCL 23DI	4.3×10^{-9}	9.6
GCL 24DI	1.6×10^{-9}	9.9
GCL 20SA	1.1×10^{-8}	7.7
GCL 21SA	1.2×10^{-8}	8.1
GCL 22SA	4.4×10^{-8}	8.2

(1) : Incomplete saturation (S_r ~ 88%).

3.2 Water retention curves

Water retention curves obtained by combining the results from the various tests are shown in Figure 2. The S_r indicated at a pressure of 0.001 MPa corresponds to the S_r calculated after the permeability tests. The open symbols correspond to results obtained with the pressure extractor and the filled points correspond to results obtained with the WP4C device. These results were fitted with the RETC software (van Genuchten et al. 2009) using the van Genuchten (vG) model (van Genuchten 1980).

The AEV of each GCL was determined by using the tangent method (Fredlund et al. 1994; Fredlund et al. 2011) on the fitted vG curve. The method is illustrated by black dashed lines in Figure 2. An AEV of ~ 0.40 MPa was obtained for the GCL permeated with DIW, and an AEV of ~ 0.25 MPa was obtained for the GCL permeated with SAMD. Furthermore, in the residual zone of the WRCs, the S_r of the GCL permeated with SAMD was generally higher than for the GCL permeated with DIW.

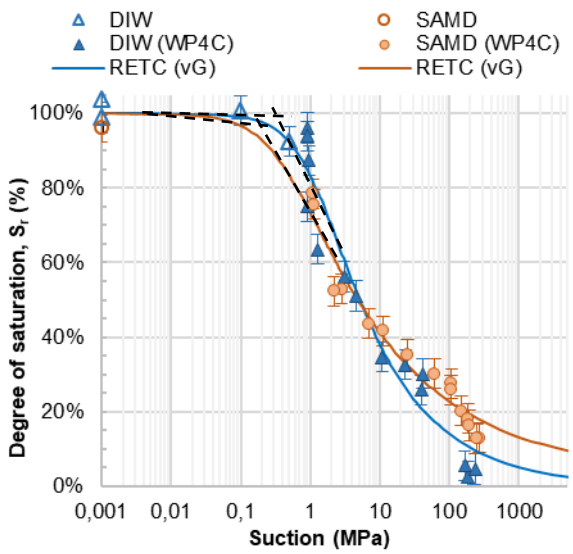

Figure 2. Water retention curves of GCL specimens permeated with DIW and SAMD

Measurements of the specimens tested in vapor desiccators were not taken at the end of the tests, and thus, the results cannot be converted in terms of an $S_r(\psi)$ relationship. However, $\omega(\psi)$ relationships for the specimen tested in the vapor desiccators and with the WP4C device followed a similar trend (Figure 3).

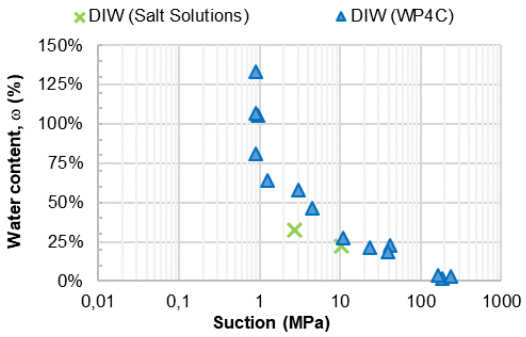

Figure 3. Comparison of results from vapor equilibrium with saturated salt solution and WP4C.

3.3 Effective diffusion coefficient

Table 3 shows the results obtained from the diffusion tests as well as the D_e values modelled with POLLUTE. The modeled D_e values are compared in Figure 4 with the D_e values predicted using the Aachib et al. (2004) model for

porosity values of 0.65 and 0.79. Modeled D_e values were similar to the predicted values for the specimens permeated with either DIW and SAMD. Smaller D_e values were obtained for the specimen with a smaller S_r.

Table 3. Oxygen diffusion test results.

Specimen	Final thickness (mm)	Porosity, n	S_r final (%)	De modelled (m^2/s)
Sand	100.5	0.40	0	3.6×10^{-6}
GCL 13DI	9.0	0.71	88	1.3×10^{-8}
GCL 18DI	10.8(1)	0.79	92	1.6×10^{-9}
GCL 20SA	7.7	0.68	92	8.4×10^{-9}
GCL 22SA	7.6	0.65	88	3.4×10^{-9}

(1) Specimen swelled during pressure plate tests

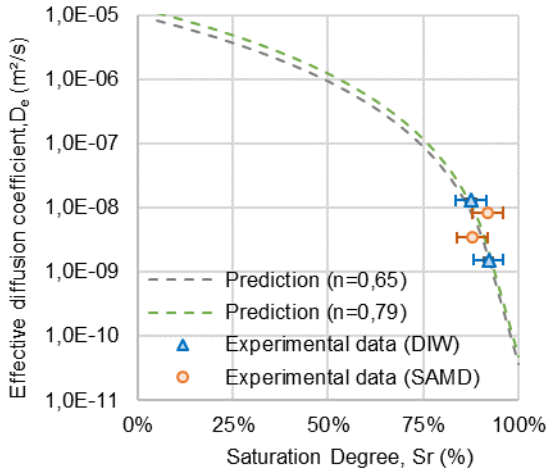

Figure 4. D_e modelled with POLLUTEv7 and estimated with Aachib et al. (2004) model.

4 DISCUSSION

4.1 Background information for interpretation of the results

Bentonite generally contains a large proportion of sodium montmorillonite (Na-Mnt). When Na-Mnt is exposed to water, two consecutive phases of hydration occur. The first phase is crystalline swelling, which starts from a dry state. During this phase, a few layers of water molecules bind to the clay sheets. The second phase is osmotic swelling. During this phase more layers of water bind to the clay sheets and they move away from each other as the number of layers increase. The pathway for free water to circulate through the Na-Mnt structure narrows and becomes more tortuous (Jo et al. 2001; Mitchell and Soga 2005; Petrov et al. 1997; Pradhan et al. 2015). This results in an increase in volume and a decrease in hydraulic conductivity.

When Na-Mnt is hydrated or permeated with a solution containing multivalent inorganic cations, the weakly bonded, monovalent Na^+ cations of the Na-Mnt are likely to be replaced by multivalent cations with greater strengths of attraction with the Mnt sheets. When only multivalent cations are present, only crystalline swelling occurs. This results in less swelling and higher hydraulic conductivities than for a Mnt hydrated with a DIW (Egloffstein 2001; Mesri and Olson 1971; Shackelford 1994; Shackelford et al. 2010; Shackelford et al. 2000).

4.2 Effects of SAMD on the k_{sat}

As shown in Table 2, permeation with SAMD resulted in a k_{sat} approximately one order of magnitude higher than that of the specimen permeated with DIW (10^{-8} cm/s for SAMD compared to 10^{-9} cm/s for DIW). Consequently, the efficiency of a GCL to act as a water barrier is adversely impacted by permeation with SAMD.

Table 2 also shows that the specimens permeated with SAMD were 15-20% thinner than those permeated with DIW (7.7-8.2 mm compared to 9.5-9.9 mm). Therefore, permeation with SAMD also reduced the swelling capacity of the GCL specimens. It is then assumed that while both crystalline and osmotic swelling occurred in the specimens permeated with DIW, little or no osmotic swelling occurred within specimens permeated by the SAMD because of cation exchanges due to the abundance of multivalent cations in the permeating liquid.

An increase in hydraulic conductivity was previously observed in the literature for GCL specimens permeated with high ionic strength and low ratio of monovalent : divalent (RMD) solutions (Jo et al. 2001; Kolstad et al. 2004; Shackelford et al. 2010), as well as for specimen permeated with strongly acidic solutions (Liu et al. 2015). In all of these cases, the increase was attributed to a loss of swelling due to cationic exchange. However, the k_{sat} values encountered in these studies were generally higher than the ones obtained in the present study, with values in the literature ranging from 10^{-7} to 10^{-5} cm/s, compared to a value of 10^{-8} cm/s in the present study. This difference could be caused by the formation of precipitates while the pH was buffered, thus resulting in pore clogging and contributed to the lower increase in hydraulic conductivity (Benson et al. 2008; Peterson and Gee 1985; Shackelford 1994).

4.3 Effects of SAMD on the WRC

One of the objectives of low k_{sat} materials in a multi-layered engineered mine cover is to limit the oxygen flux reaching the underlying wastes by maintaining a high S_r. The higher the AEV of a material, the higher its resistance is to desaturation. As shown in Figure 2, the AEVs of GCLs permeated with SAMD and DIW are estimated to be 0.25 MPa and 0.40 MPa, respectively. However, for the GCL permeated with SAMD, the estimated AEV value is based on a limited set of measurements in the 0-1 MPa suction range. More data points would improve the WRC in this range of suctions and enable better conclusions on the impact of the permeating liquid on the AEV. Nevertheless, the obtained results indicate that the AEVs of GCLs permeated with SAMD and with DIW are both relatively high.

Figure 2 shows that, in the residual zone ($S_r < 40\%$ and $\psi > 20$ MPa), the permeating liquid influenced the $S_r(\psi)$ relationship. A similar observation was made by Yesiller et al. (2014) for $\omega(\psi)$ relationships. At these low S_r values, generally only crystalline hydration occurs (Mooney et al.

1952; Scalia IV and Benson 2011). In the present study, the water content was similar for the specimens permeated with SAMD and DI at the same suction, thus indicating similar hydration around the clay sheets. However, the void volumes of specimens permeated with DIW were always greater than that of specimen permeated with SAMD for a given suction (detailed results presented in Chevé, 2019). This generally results in a smaller S_r for the specimen permeated with DIW.

4.4 Effects of SAMD on the D_e

The use of SAMD instead of DIW to permeate GCL specimens was hypothesized to impact two parameters in the D_e equation (Equation 2): Henry's constant (H) and the free diffusion coefficient of O_2 in the liquid phase (D_w^0). This is because salinity decreases the amount of O_2 that can be dissolved in a liquid (Benson and Krause 1980; Benson and Krause Jr 1984; Meyers 2011), as well as the ability of the O_2 to diffuse. This results in lower *H* and D_w^0 values for SAMD, thus lower D_e. Although the salinity of the SAMD is non-negligible, the magnitude of the changes that it induces on the D_e are in the order of 10^{-11} m²/s for the tests carried out, which is smaller than the precision of the method. This is consistent with the results illustrated in Figure 4, which shows no differences between the permeating liquids, and where measured D_e values generally agree with predicted D_e values.

Aubertin et al. (2000) determined the D_e of GCL specimens containing 3300 g/m² of bentonite (nominal value) that were fully saturated with DIW. Measured D_e values of ~10^{-11} m²/s were obtained, and also corresponded well with values predicted using the Aachib et al. (2004) model.

As indicated in Equation 1, the diffusive oxygen flux (F) through a porous material is related to the oxygen concentration gradient. Although the D_e was not significantly influenced by permeation with SAMD, O_2 fluxes were greater through a GCL specimen permeated with SAMD because the GCL was thinner and, consequently, undergo larger O_2 gradient.For a GCL with a S_r ~ 92% (D_e of 10^{-9} m²/s; Figure 4) placed over reactive tailings and under steady-state conditions (O_2 concentration below and above the GCL of 0 and 270 g/m³, respectively; Aubertin et al. 2000), the annual fluxes for thicknesses of 8.0 mm and 9.5 mm would be of 1185 g O_2/yr and 995 g O_2/yr, respectively. Thus, the performance of a GCL as an oxygen barrier in an engineered cover is adversely impacted by permeation with SAMD. However, these annual fluxes are significantly greater than the values that are generally targeted for an efficient oxygen barrier (25-50 g O_2/yr) (Aubertin et al. 2000).

5 SUMMARY AND CONCLUSION

The present study was conducted to determine the effects of permeation with SAMD on a conventional GCL, in particular with respect to the properties of interest for a low-permeability layer in a multi-layered engineered mine waste cover installed over reactive mine waste. Saturated hydraulic conductivities, water retention curves, and effective diffusion coefficients were determined in laboratory for GCL specimens saturated with DIW and SAMD under low confining pressures.

The investigation showed that permeation with SAMD adversely impacted the k_{sat} of the studied GCL (10^{-8} cm/s and 10^{-9} cm/s for SAMD and DIW, respectively) and the thickness of the material at saturation (average of 8.0 mm and 9.7 mm for SAMD and DIW). These differences were attributed to cation exchanges that occurred during permeation with SAMD that likely prevented the osmotic hydration of the bentonite and limited its swelling capacity.

Permeation with SAMD did not seem to influence the AEV of the GCL, but additional investigations in the 0-1 MPa suction range must be conducted to clarify these results. However, a difference was observed in the residual zone of the WRC, where, for a given suction, the S_r values of the specimens permeated with SAMD were higher than those of specimens permeated with DIW. Although permeation with SAMD could theoretically also impact the D_e of the material, these impacts were too small to be measured with the applied methods, and similar D_e values were obtained both for permeation with DIW and SAMD. Because the GCLs hydrated with SAMD were usually thinner, a larger oxygen flux would occur through a GCL permeated with SAMD for a given D_e.

The performance of a GCL in an engineered multi-layer cover installed over reactive mine wastes, both as a water and oxygen barrier, could be adversely affected by hydration with AMD The results presented in this paper are specific to the combination of the GCL and SAMD used in this experiment and for ideal laboratory conditions. More work is needed to validate these laboratory observations with in situ samples that are exposed to field conditions.

ACKNOWLEDGEMENTS

Financial support for this study was provided by the Natural Sciences and Engineering Research Council of Canada through the NSERC-UQAT Industrial Research Chair on mine site reclamation and by the industrial partners of the Research Institute on Mines and the Environment (RIME) UQAT-Polytechnique. The authors also express their appreciation to Gary Schudel from the Université du Québec en Abitibi-Témiscamingue for his constructive comments on the manuscript

REFERENCES

Aachib, M., Aubertin, M., and Mbonimpa, M. Laboratory measurements and predictive equations for gas diffusion coefficient of unsaturated soils. *In* Proceedings of the 55th Canadian Geotechnical Conference and 3rd joint IAH-CNC and CGS Groundwater Specialty Conference, Niagara Falls, Ont. 2002. pp. 20-23.

Aachib, M., Mbonimpa, M., and Aubertin, M. 2004. Measurement and prediction of the oxygen diffusion coefficient in unsaturated media, with applications to soil covers. Water, Air, and Soil Pollution, **156**(1): 163-193.

Akcil, A., and Koldas, S. 2006. Acid mine drainage (AMD): causes, treatment and case studies. Journal of cleaner production, **14**(12-13): 1139-1145.

ASTM. 2012. D6766-12 Standard Test Method for Evaluation of Hydraulic Properties of Geosynthetic Clay Liners Permeated with Potentially Incompatible Aqueous Solutions. American Society for Testing and Materials International, West Conshohocken, Pennsylvania, USA.

ASTM. 2014. D5550-14 Standard Test Method for Specific Gravity of Soil Solids by Gas Pycnometer. American Society for Testing and Materials International, West Conshohocken, Pennsylvania, USA.

ASTM. 2016. D5887 /D5887M-16 Standard Test Method for Measurement of Index Flux Through Saturated Geosynthetic Cly Liner Specimens Using a Flexible Wall Permeameter. American Society for Testing and Materials International, West Conshohocken, Pennsylvania, USA.

Aubertin, M., Aachib, M., and Authier, K. 2000. Evaluation of diffusive gas flux through covers with a GCL. Geotextiles and Geomembranes, **18**(2–4): 215-233.

Aubertin, M., Bussière, B., Pabst, T., James, M., and Mbonimpa, M. 2016. Review of the reclamation techniques for acid-generating mine wastes upon closure of disposal sites. *In* Geo-Chicago 2016. pp. 343-358.

Benson, B.B., and Krause, D. 1980. The concentration and isotopic fractionation of gases dissolved in freshwater in equilibrium with the atmosphere. 1. Oxygen. Limnology and Oceanography, **25**(4): 662-671.

Benson, B.B., and Krause Jr, D. 1984. The concentration and isotopic fractionation of oxygen dissolved in freshwater and seawater in equilibrium with the atmosphere 1. Limnology and Oceanography, **29**(3): 620-632.

Benson, C., Wang, X., Gassner, F., and Foo, D. 2008. Hydraulic conductivity of two geosynthetic clay liners permeated with an aluminum residue leachate. GeoAmericas 2008, International Geosynthetics Society.

Blowes, D.W., Ptacek, C.J., Jambor, J.L., Weisener, C.G., Paktunc, D., Gould, W.D., and Johnson, D.B. 2014. 11.5 - The Geochemistry of Acid Mine Drainage. *In* Treatise on Geochemistry (Second Edition). *Edited by* H.D. Holland and K.K. Turekian. Elsevier, Oxford. pp. 131-190.

Bouazza, A. 2002. Geosynthetic clay liners. Geotextiles and Geomembranes, **20**(1): 3-17.

Bruker, A. 2009. Topas V4. 2: General profile and structure analysis software for powder diffraction data. Bruker AXS, Karlsruhe, Germany.

Chevé, N. 2019. Évaluation de la performance de géocomposites bentonitiques comme barrière aux fluides dans un contexte de recouvrement minier. Mineral Engineering Master thesis, Polytechnique Montréal, offered in extension at Université du Québec en Abitibi-Temiscamingue.

Collin, M. 1987. Mathematical modeling of water and oxygen transport in layered soil covers for deposits of pyritic mine tailings. Licenciate Treatise. Royal Institute of Technology. Department of Chemical Engineering. S-10044 Stockholm, Sweden.

Conzelmann, J., Scalia IV, J., and Shackelford, C.D. 2017. Effect of Backpressure Saturation on the Hydraulic Conductivity of GCLs. *In* Geotechnical Frontiers 2017. pp. 227-235.

Crank, J. 1975. The mathematics of difiusion. 2nd end.

Cussler, E.L. 2009. Diffusion: mass transfer in fluid systems. Cambridge University Press.

Daniel, D.E., Bowders, J.J., and Gilbert, R.B. 1997. Laboratory hydraulic conductivity testing of GCLs in flexible-wall permeameters. *In* Testing and acceptance criteria for geosynthetic clay liners. ASTM International.

Devices, D. 2010. WP4C Dewpoint PotentiaMeter operator's manual, Version 2. Decagon Devices, Pullman, WA.

Egloffstein, T.A. 2001. Natural bentonites—influence of the ion exchange and partial desiccation on permeability and self-healing capacity of bentonites used in GCLs. Geotextiles and Geomembranes, **19**(7): 427-444.

Eigenbrod, K. 2003. Self-healing in fractured fine-grained soils. Canadian Geotechnical Journal, **40**(2): 435-449.

Fredlund, D., Xing, A., and Huang, S. 1994. Predicting the permeability function for unsaturated soils using the soil-water characteristic curve. Canadian Geotechnical Journal, **31**(4): 533-546.

Fredlund, D.G., Sheng, D., and Zhao, J. 2011. Estimation of soil suction from the soil-water characteristic curve. Canadian Geotechnical Journal, **48**(2): 186-198.

INAP. 2012. Global Acid Rock Drainage Guide. Available from http://www.gardguide.com [accessed March 2019.

Jo, H.Y., Katsumi, T., Benson, C.H., and Edil, T.B. 2001. Hydraulic conductivity and swelling of nonprehydrated GCLs permeated with single-species salt solutions. Journal of Geotechnical and Geoenvironmental Engineering, **127**(7): 557-567.

Koerner, G.R. Geosynthetic Institute's Efforts In Accreditation and Certification. *In* Proceedings of Symposium Honoring the Research Achievement of Dr. Robert M. Koerner, Philadelphia, PA, GII Press. 2004. pp. 204-215.

Kolstad, D.C., Benson, C.H., and Edil, T.B. 2004. Hydraulic conductivity and swell of nonprehydrated geosynthetic clay liners permeated with multispecies inorganic solutions. Journal of Geotechnical and Geoenvironmental Engineering, **130**(12): 1236-1249.

Lange, K., Rowe, R., and Jamieson, H. 2007. Metal retention in geosynthetic clay liners following permeation by different mining solutions. Geosynthetics International, **14**(3): 178-187.

Lindsay, M.B.J., Moncur, M.C., Bain, J.G., Jambor, J.L., Ptacek, C.J., and Blowes, D.W. 2015. Geochemical and mineralogical aspects of sulfide mine tailings. Applied Geochemistry, **57**: 157-177.

Liu, Y., Bouazza, A., Gates, W.P., and Rowe, R.K. 2015. Hydraulic performance of geosynthetic clay liners to sulfuric acid solutions. Geotextiles and Geomembranes, **43**(1): 14-23.

Lu, Y., Abuel-Naga, H., and Bouazza, A. 2017. Water retention curve of GCLs using a modified sample holder in a chilled-mirror dew-point device. Geotextiles and Geomembranes, **45**(1): 23-28.

Makusa, G.P., Bradshaw, S.L., Berns, E., Benson, C.H., and Knutsson, S. 2014. Freeze–thaw cycling concurrent with cation exchange and the hydraulic conductivity of geosynthetic clay liners. Canadian Geotechnical Journal, **51**(6): 591-598.

Mbonimpa, M., Aubertin, M., and Bussière, B. 2006. Predicting the unsaturated hydraulic conductivity of granular soils from basic geotechnical properties using the modified Kovács (MK) model and statistical models. Canadian Geotechnical Journal, **43**(8): 773-787.

Mbonimpa, M., Aubertin, M., Buissière, B., and Aachib, M. 2002. Oxygen diffusion and consumption in unsaturated cover materials.

Meer, S.R., and Benson, C.H. 2007. Hydraulic conductivity of geosynthetic clay liners exhumed from landfill final covers. Journal of Geotechnical and Geoenvironmental Engineering, **133**(5): 550-563.

Melchior, S. Field studies and excavations of geosynthetic clay barriers in landfill covers. *In* Clay Geosynthetics Barriers, Proceedings of the international symposium IS Nuremberg. 2002. pp. 321-330.

Mesri, G., and Olson, R.E. 1971. Mechanisms Controlling the Permeability of Clays.

Meyers, D. 2011. Office of Water Quality Technical Memorandum 2011.03: Analysis to Support the Replacement of Weiss (1970) Equations by Benson and Krause (1980, 1984) Equations for USGS Computation of Solubility of Dissolved Oxygen in Water. Office of Water Quality, Reston, VA, USA.

Mitchell, J.K., and Soga, K. 2005. Fundamentals of soil behavior. John Wiley & Sons New York.

Moncur, M., Ptacek, C., Blowes, D., and Jambor, J. 2005. Release, transport and attenuation of metals from an old tailings impoundment. Applied Geochemistry, **20**(3): 639-659.

Mooney, R., Keenan, A., and Wood, L. 1952. Adsorption of water vapor by montmorillonite. II. Effect of exchangeable ions and lattice swelling as measured by X-ray diffraction. Journal of the American Chemical Society, **74**(6): 1371-1374.

Peterson, S.R., and Gee, G.W. 1985. Interactions between acidic solutions and clay liners: permeability and neutralization. *In* Hydraulic Barriers in Soil and Rock. ASTM International.

Petrov, R.J., Rowe, R.K., and Quigley, R.M. 1997. Selected factors influencing GCL hydraulic conductivity. Journal of Geotechnical and Geoenvironmental Engineering, **123**(8): 683-695.

Pradhan, S.M., Katti, K.S., and Katti, D.R. 2015. Evolution of Molecular Interactions in the Interlayer of Na-Montmorillonite Swelling Clay with Increasing Hydration. International Journal of Geomechanics, **15**(5).

Rouf, M.A., Singh, R.M., Bouazza, A., Rowe, R.K., and Gates, W.P. 2016. Gas permeability of partially hydrated geosynthetic clay liner under two stress conditions. Environmental Geotechnics, **3**(5): 325-333. doi:10.1680/envgeo.14.00009.

Rowe, R.K., and Hosney, M.S. 2013. Laboratory investigation of GCL performance for covering arsenic contaminated mine wastes. Geotextiles and Geomembranes, **39**: 63-77.

Sari, K., and Chai, J. 2013. Self healing capacity of geosynthetic clay liners and influencing factors. Geotextiles and Geomembranes, **41**: 64-71.

Scalia IV, J., and Benson, C.H. 2011. Hydraulic conductivity of geosynthetic clay liners exhumed from landfill final covers with composite barriers. Journal of Geotechnical and Geoenvironmental Engineering, **137**(1): 1-13.

Scalia, J., and Benson, C.H. 2010. Preferential flow in geosynthetic clay liners exhumed from final covers with composite barriers. Canadian Geotechnical Journal, **47**(10): 1101-1111.

Shackelford, C.D. 1994. Waste-soil interactions that alter hydraulic conductivity. *In* Hydraulic conductivity and waste contaminant transport in soil. ASTM International.

Shackelford, C.D., Sevick, G.W., and Eykholt, G.R. 2010. Hydraulic conductivity of geosynthetic clay liners to tailings impoundment solutions. Geotextiles and Geomembranes, **28**(2): 149-162.

Shackelford, C.D., Benson, C.H., Katsumi, T., Edil, T.B., and Lin, L. 2000. Evaluating the hydraulic conductivity of GCLs permeated with non-standard liquids. Geotextiles and Geomembranes, **18**(2–4): 133-161.

Sivakumar Babu, G.L., Sporer, H., Zanzinger, H., and Gartung, E. 2001. Self-Healing Properties of Geosynthetic Clay Liners. Geosynthetics International, **8**(5): 461-470.

van Genuchten, M. 1980. A closed-form equation for predicting the hydraulic conductivity of unsaturated soils. Soil Science Society of America Journal, **44**(5): 892-898.

van Genuchten, M.T., Simunek, F., Leij, F., and Sejna, M. 2009. The RETC code (version 6.02) for quantifying the hydraulic functions of unsaturated soils.

Wexler, A., and Hasegawa, S. 1954. Relative humidity-temperature relationships of some saturated salt solutions in the temperature range 0 to 50 C. Journal of Research of the National Bureau of Standards, **53**(1): 19-26.

Wijaya, M., Leong, E.C., and Rahardjo, H. 2015. Effect of shrinkage on air-entry value of soils. Soils and foundations, **55**(1): 166-180.

Yesiller, N., Risken, J., Hanson, J., and Darius, J. 2014. Effects of Hydration Fluid on Moisture-Suction Relationships for Geosynthetic Clay Liners. Proceedings UNSAT2014.

Young, J.F. 1967. Humidity control in the laboratory using salt solutions—a review. Journal of Applied Chemistry, **17**(9): 241-245.